

## Reply to Referee #1:

Dear Reviewer: Thank you for your comments. Our responses to the comments are listed below:

*(1) How the soil water storage is determined? It varies at seasonal scale. How does it will affect your analysis? It is worth to highlight following article that developed a three parameter streamflow elasticity model as a function of precipitation, potential evaporation, and change in groundwater storage applicable at both seasonal and annual scales. <https://hess.copernicus.org/articles/20/2545/2016/>*

Thank you for the comment. Soil water storage capacity in this study is referred to as the maximum storage capacity from the land surface to the bedrock; therefore, it is considered as a static variable. The effective storage capacity or the remaining storage capacity could vary temporally due to the dynamics of groundwater storage as shown in *Konapala and Mishra (2016)*. The definition of the soil water storage capacity has been clarified on Lines 60-61 in the revised manuscript:

Lines 60-61: “Soil water storage capacity is the maximum storage capacity from land surface to bedrock, which exerts a powerful control on mean annual runoff (Konapala and Mishra, 2016).”

“Konapala, G., and Mishra, A. K.: Three-parameter-based streamflow elasticity model: Application to MOPEX basins in the USA at annual and seasonal scales., *Hydrol. Earth Syst. Sci.*, 20, 2545-2556, <https://doi.org/10.5194/hess-20-2545-2016>.”

*(2) What do mean by Climate variability in your study? does it mean distribution of climate variables, for example, distribution of rainy days within the season. This type of analysis are important and they have a direct influence on the soil water storage. This can be discussed as a scope of the future work. The magnitude and seasonality of the climate variables affects water availability (storage). This may be included as a future scope of the work. Please see this article: <https://www.nature.com/articles/s41467-020-16757-w>*

Thank you for the comment. Following *Yao et al. (2020)*, the climate variability in this study is defined as the temporal variations of precipitation ( $P$ ) and potential evapotranspiration ( $E_p$ ), including their intra-monthly, intra-annual, and inter-annual variations. For example, the deviations of daily  $P$  or  $E_p$  from its monthly mean values are defined as the intra-monthly variations. The definition of climate variability has been included in the revised manuscript on Lines 113-118. In addition, we totally agree with you that the distribution of rainy days, the magnitude and the seasonality of climate variables have direct impacts on soil water storage, and

we have included them as a scope of our future work on Lines 392-395 in the revised manuscript:

Lines 113-118: “Climate variability is defined as the temporal variations of precipitation ( $P$ ) and potential evapotranspiration ( $E_p$ ), including their intra-monthly, intra-annual, and inter-annual variations. For example, the deviations of daily  $P$  or  $E_p$  from its monthly mean values are defined as the intra-monthly variations (Yao et al., 2020). As discussed in the Introduction section, the mean annual runoff model takes daily precipitation and potential evaporation as inputs, therefore, climate variability is explicitly included in the model.”

“Yao, L., Libera, D. A., Kheimi, M., Sankarasubramanian, A., and Wang, D (2020): The roles of climate forcing and its variability on streamflow at daily, monthly, annual, and long-term scales. *Water Resour. Res.*, 55, e2020WR027111. <https://doi.org/10.1029/2020WR027111>.”

Lines 392-395: “Future research will investigate alternative methods for better estimating the spatial variability of soil water storage capacity over watersheds, and quantify the impacts of vegetation and climate variability (e.g., distribution of rainy days, the magnitude and the seasonality of climate variables).”

*(3) Are you using SCS method to find the infiltration loss? Does this loss is connected to shallow water storage?*

Yes. Infiltration loss is computed by Equation (2) which leads to the proportionality relationship of SCS method. The value of infiltration loss is dependent on the shallow water storage condition, which affects the remaining storage capacity. The “normal antecedent moisture” in the SCS curve number method is treated as the storage at the long-term steady-state condition. Therefore, the maximum storage capacity is the sum (Equation (7)) of storage capacity computed by the SCS curve number (Equation (6)) and long-term average storage.

*(4) Baseflow plays an important role in the runoff analysis. Are you including this factor in your analysis. Can addition of the seasonal baseflow characteristics will improve the results?*

We agree that baseflow plays an important role in total runoff which includes baseflow and surface runoff. However, this research is focused on total runoff; therefore, baseflow is not explored separately in this study. On the other hand, the seasonal characteristics of baseflow are results of climate seasonality, which is implicitly included in the daily climate input. This has been clarified on Lines 153-155 in the revised manuscript:

Lines 153-155: “Note that the mean annual runoff includes surface runoff and baseflow, and both are impacted by climate variability (e.g., intra-annual variability) (Berghuijs et al., 2014; Fan et al., 2007).”

“Fan, Y., Miguez-Macho, G., Weaver, C. P., Walko, R., and Robock, A: Incorporating water table dynamics in climate modeling: 1. Water table observations and equilibrium water table simulations, *J. Geophys. Res.*, 112, D10125, doi:10.1029/2006JD008111, 2007.

Berghuijs, W. R., Sivapalan, M., Woods, R. A., and Savenije, H. H.: Patterns of similarity of seasonal water balances: A window into streamflow variability over a range of time scales, *Water Resour. Res.*, 50(7), 5638-5661, <https://doi.org/10.1002/2014WR015692>, 2014.”

*(5) How the curve numbers are derived? Did you derive the composite curve numbers, i.e., one value for a watershed?*

Yes, each watershed has one curve number, which is the average curve number over the grid cells within the entire watershed. For each grid cell, the curve number is obtained based on land use and land cover and hydrologic soil group as introduced in Section 2.2.1. The composite curve number for each watershed has been clarified in the revised manuscript:

Lines 175-176: “where CN is the composite curve number based on land use and land cover (LULC) and hydrologic soil group (HSG) for each watershed.”

*(6) How the bedrock topography are determined?*

The bedrock topography data of the study catchments are not available from observations in this study; therefore, we used a hypothetical bedrock topography obtained through Height Above the Nearest Drainage (HAND) method which assumes that the bedrock of each hillslope is horizontal and the bedrock elevation equals the elevation of the drainage point. This has been clarified on Lines 354-355 in the revised manuscript:

Lines 354-355: “This is due to the assumption of the HAND method that the bedrock between a specific point and its nearest drainage point is horizontal and intercepts with the channel bed.”

*(7) I assume the shape parameter is kept constant for a given watershed, and it is calculated based by creating a time series based on the spatial (gridded) soil water capacity values. How the shape parameters are calculated? For example, Maximum Likelihood methods?? Do you think the parameter uncertainty (range) will affect the mean flow?*

Yes, the shape parameter is kept constant for a given watershed. While, it is calculated by creating the spatial soil water capacity values under the long-term averaged antecedent soil moisture condition. A nonlinear programming solver using derivative-free method, i.e., Matlab function “fminsearch”, was used to calculate the optimal shape parameter by minimizing the root mean square error (RMSE). The method has been clarified on Lines 227-230 in the revised manuscript. For the parameter uncertainty, its impact on the mean annual runoff can be seen by comparing Figures 5a and 5c. The value of the average soil water storage capacity of each

catchment is same between these two figures, and the different simulation performance is only caused by the shape parameter. Clearly, the shape parameter could largely affect the mean annual runoff. In the revise manuscript, the sensitivity of mean annual runoff to the shape parameter has been conducted, and is shown in the new figure, i.e., Figure 2, and the clarification has been added on Lines 230-238 in the revised manuscript:

Lines 227-230: “The shape parameter  $a$  is then estimated by fitting the point-scale storage capacity data obtained from Equation (11). A nonlinear programming solver using derivative-free method (i.e., Matlab function “fminsearch”) was used to calculate the optimal shape parameter by minimizing the root mean square error (RMSE).”

Lines 230-238: “To demonstrate the sensitivity of mean annual runoff to the value of shape parameter, Figure 2 presents mean annual runoff versus shape parameter based on the mean annual water balance (Yao et al., 2020). It can be found that mean annual runoff decreases significantly as shape parameter increases, especially when shape parameter approaches its upper limit (i.e., 2). The negative relationship between mean annual runoff and shape parameter can be attributed to the fact that the larger shape parameter indicates that less watershed area has small values of point-scale storage capacity (Wang, 2018) and more precipitation could be retained underground for evaporation.”

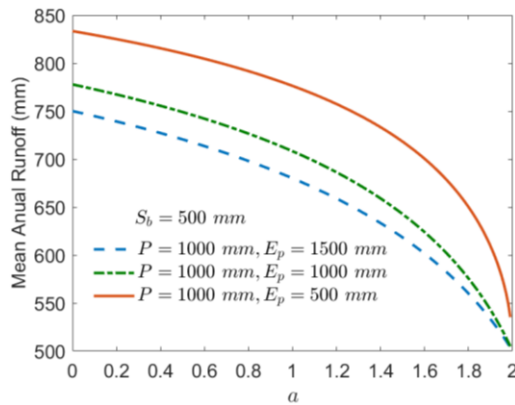


Figure 2: The sensitivity of mean annual runoff ( $Q$ ) to the value of shape parameter ( $a$ ).

(8) Line 98-100: Can be revised to make it simple.

Thanks. This sentence has been revised on Lines 104-107 in the revised manuscript:

“The mean soil water storage capacity is estimated from curve number and climate because

soil water storage capacity consists of the antecedent soil water storage and the potential maximum soil moisture retention which can be calculated through SCS curve number method.”

## Reply to Referee #2:

*This manuscript tried to parameterize the two parameters of the mean annual balance equation by relating their values with the controlling factors, in order to develop a model to estimate mean annual runoff in ungauged basins. It is an interesting topic and suitable for HESS. However, I have several comments as follow.*

Thank you very much for your comments and suggestions. Our replies are listed as follow:

*(1) It isn't clear which equation is the water balance model that was developed for estimating mean annual runoff.*

Thank you for pointing out the problem. The mean annual runoff is computed by the difference of mean annual precipitation and mean annual evaporation which is computed by aggregating the daily evaporation calculated by Equation (3). This has been clarified and the equation for mean annual runoff has been presented explicitly on Lines 147-153 in the revised manuscript:

Lines 147-153: "Mean annual evaporation ( $\bar{E}$ ) is computed by aggregating the daily evaporation, and mean annual runoff ( $\bar{Q}$ ) is computed as the difference of mean annual precipitation and evaporation:

$$\bar{E} = \frac{\sum_{y=1}^Y \sum_{d=1}^{D_y} E_d}{Y} \quad (4)$$

$$\bar{Q} = P - \bar{E} \quad (5)$$

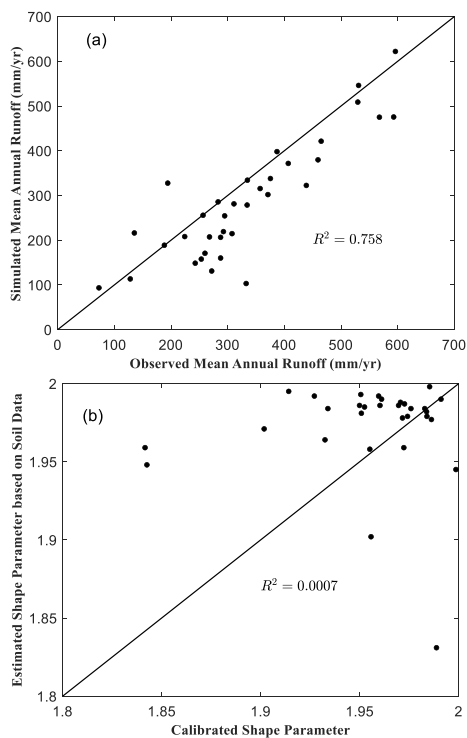
where,  $Y$  is the number of years, and  $D_y$  is the number of days in  $y^{\text{th}}$  year;  $y$  and  $d$  represent the  $y^{\text{th}}$  year and  $d^{\text{th}}$  day, respectively."

*(2) As shown in Figure 5(b), there is a large difference and low correlation between the estimated shape parameter and the calibrated one. At the same time, Figure 5(a) shows that the model has a fair estimation of mean annual runoff with the estimated shape parameter. I guess that the model has a low sensitivity to the shape parameter. I suggest a sensitivity analysis on the parameter. Also, it is necessary to evaluate the improvement due to the parameterization from soil characteristics as given in Section 2.2.2, since it is a relatively complicated process. In addition, I suggest that some statistical indicators should be given in Figure 5. 3.*

Thank you for your suggestion. The narrow ranges of the axes may give us the impression that the difference between the estimated shape parameter and the calibrated one are large, while actually the mean difference is 0.06 which is small considered that the range of the shape parameter is from 0 to 2. The sensitivity analysis of the mean annual runoff to the shape parameter has been conducted and shown in the new figure (i.e., Figure 2), and the clarification has been added on Lines 230-238 in the revised manuscript. The coefficients of determination ( $R^2$ ) have been calculated for Figure 6 (Figure 5 in the original version) in the revised manuscript. For the parameterization in Section 2.2.2, it is a new method proposed in this study to quantify the spatial heterogeneity of the soil water storage capacity, which is then discussed in Section 3 on how to improve the estimation by considering more details of the bedrock information, therefore, the focus

of this study is not the improvement of the shape parameter parameterization from the soil characteristics.

Lines 230-238: “To demonstrate the sensitivity of mean annual runoff to the value of shape parameter, Figure 2 presents mean annual runoff versus shape parameter based on the mean annual water balance (Yao et al., 2020). It can be found that mean annual runoff decreases significantly as shape parameter increases, especially when shape parameter approaches its upper limit (i.e., 2). The negative relationship between mean annual runoff and shape parameter can be attributed to the fact that the larger shape parameter indicates that less watershed area has small values of point-scale storage capacity (Wang, 2018) and more precipitation could be retained underground for evaporation.”



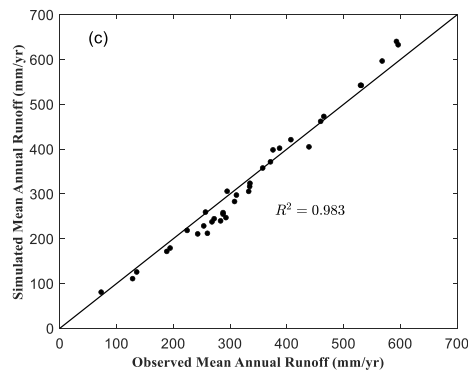


Figure 6: (a) Observed versus simulated mean annual runoff using shape parameter based on soil data; (b) Soil data-based versus calibrated shape parameter; and (c) Observed versus simulated mean annual runoff using shape parameter based on calibration.

*(3) In Lines 142-148, the authors pointed out the effect of climate variability on water balance, but it isn't clear how to deal with the effect of climate variability in the developed model. In addition, previous studies reported that many factors, such as vegetation, catchment slope and etc., have an impact on water balance. I am not sure whether such factors have more larger impact on water balance than the spatial variability of storage capacity has. There is a possibility that their impacts can be attributed to the impact of the distribution of soil water storage capacity. More analysis and discussions are required.*

We are sorry for the confusion. Different from traditional mean annual water balance models which take the mean annual precipitation ( $P$ ) and potential evapotranspiration ( $E_p$ ) as climate inputs, our model is forced by the observed daily  $P$  and  $E_p$ ; therefore, the effects of the climate variability, including the intra-monthly, intra-annual, and inter-annual climate variability are explicitly included. In the revised manuscript, we have clarified how to deal with the effect of climate variability when we introduce the structure of the developed model in Section 2.1 (Lines 113-118). For the other factors such as vegetation and catchment slope, we agree that their impacts can attribute to the distribution of soil water storage capacity as a result of catchment coevolution. The land surface topography (i.e., DEM) is one of the controlling factors for determining the soil thickness in this study; therefore, the topographic characteristics including the catchment slope has been considered through DEM data. To further explore the impact of catchment topographic features, we have added a discussion on determining the shape parameter of the soil storage capacity through the spatial variability of the topographic wetness index in Lines 340-347 and 359-364 in the revised manuscript. For the impact of vegetation on the soil water storage capacity distribution, it has been included as a future scope of our work on Lines 392-395 in the revised manuscript:



Lines 113-118: “Climate variability is defined as the temporal variations of precipitation ( $P$ ) and potential evapotranspiration ( $E_p$ ), including their intra-monthly, intra-annual, and inter-annual variations. For example, the deviations of daily  $P$  or  $E_p$  from its monthly mean values are defined as the intra-monthly variations (Yao et al., 2020). As discussed in the Introduction section, the mean annual runoff model takes daily precipitation and potential evaporation as inputs, therefore, climate variability is explicitly included in the model.”

Lines 340-347: “The control of land surface topography on the hydrologic process has also been widely quantified through topographic wetness index (TWI) of TOPMODEL (Beven and Kirkby, 1979). The spatial variability of soil storage capacity based on the TOPMODEL assumption has been demonstrated as a beneficial representation of the conceptual model (Sivapalan et al., 1997). Therefore, the heterogeneity of TWI in a watershed was proposed to be another surrogate of the heterogeneity of the soil storage capacity in this study, and the shape parameter estimated by fitting TWI against Equation (12) through minimizing the root mean square error (RMSE) for the Maquoketa River in Iowa was compared with those obtained from other methods.”

Lines 359-364: “The dashed dot red line in Figure 7 displays the CDF of the normalized soil storage capacity based on TWI, and the corresponding value of  $a$  is 1.967. The TWI-based  $a$  value also presents a larger spatial variability than that derived from soil data solely, confirming the importance of topography in determining the heterogeneity of soil water storage capacity. The deviation of the TWI-based  $a$  value from its calibrated counterpart could be due to the fact that the bedrock topography is not considered in TWI.”

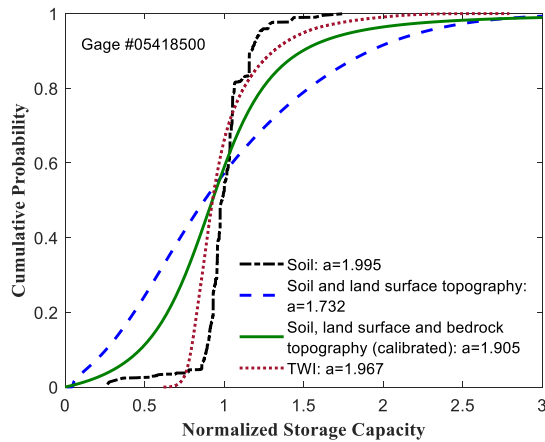


Figure 7: The effects of soil, land surface topography, bedrock topography, and topographic wetness index (TWI) on the shape parameter of the spatial distribution of soil water storage capacity.

Lines 392-395: “Future research will investigate alternative methods for better estimating the spatial variability of soil water storage capacity over watersheds, and quantify the impacts of vegetation and climate variability (e.g., distribution of rainy days, the magnitude and the seasonality of climate variables).”

**Reply to Referee #3:**

*Wang and Gao et al conducted a study to develop a nonparametric mean annual water balance model for prediction in ungauged basins. They found that climate and topography play essential roles determining the storage capacity and its shape. I found this study is quite interesting and fits the scope of HESS. Relevant studies should be encouraged to understand and diagnose the impacts of different features on runoff generation in different time scales and their connections. Here I have several comments for the authors to consider for further improving the quality:*

We thank the reviewer for this positive feedback. Our responses to your comments are listed below.

*(1) Why did the authors only use 35 catchments in this study? There are over 400 catchments in MOPEX data. Please clarify the reasons to exclude most catchments.*

The 35 watersheds are selected considering the data availability including soil (hydrologic soil group), land cover and land use, DEM as well as the minimum snow effect and human activities. The data processing demand is also a consideration for selecting the limited number of watersheds. We think that the number of watersheds is sufficient for diagnosing the data requirement for estimating long-term runoff in ungauged basins, for example, the importance of bedrock data. The reasons have been clarified in the revised manuscript on Lines 240-244:

“The number of 35 was determined due to the consideration of the data availability including soil (hydrologic soil group), land cover and land use, DEM as well as the minimum snow effect and human activities (Wang and Hejazi, 2011), and to keep the efforts of gSSURGO data processing to a reasonable level while still to have a sufficient number of sample of catchments.”

*(2) Line 73-74. I cannot follow this sentence. Please rephrase it.*

Thank you for pointing out the problem. This sentence has been revised on Line 74-80 in the revised manuscript:

“It has also been suggested that the spatial variability of soil water storage capacity could suppress the actual evaporation because the maximum evaporation in areas with soil water storage capacity less than  $E_p$  will be smaller than  $E_p$ ; therefore, the average evaporation over the entire catchment is smaller than  $E_p$  even though the average storage is greater than  $E_p$ , resulting in more runoff generation compared to the situation when the soil water storage capacity is spatially uniform (Yao et al., 2020).”

*(3) Line 243. The  $S_b$  in Chattahoochee River watershed reaches to 1870mm. The value is too large, which let me doubt the physical meaning of the  $S_b$  parameter.*

Sorry for the typo on the number of  $S_b$  in Chattahoochee River, and it should be 1559 mm. The value has been corrected on Lines 275-277 in the revised manuscript. The physical meaning of  $S_b$  is the mean value of the soil water storage capacity over a catchment which is defined as the maximum storage from land surface to bedrock in this study rather than the storage capacity from shallow soils. Considering the maximum of soil water storage capacity could be 2000 mm from literature (Kollat *et al.*, 2012), 1559 mm is considered to be reasonable in this study. The definition of the  $S_b$  has been clarified in the revised manuscript on Lines 187-189.

Lines 275-277: “As shown in Table 1, the estimated  $S_b$  varies from 177 mm (Chikaskia River watershed) to 1559 mm (Chattahoochee River watershed) over the study watersheds.”

Lines 187-189: “The physical meaning of  $S_b$  is the mean value of the soil water storage capacity over a watershed which is defined as the maximum storage from land surface to bedrock in this study rather than the storage capacity from shallow soils.”

Kollat, J., Reed, P. M., and Wagener, T.: When are multiobjective calibration trade-offs in hydrologic models meaningful?, *Water Resour. Res.*, 48(3) <https://doi.org/10.1029/2011WR011534>.

1                   **Diagnosis toward predicting mean annual runoff in ungauged basins**

2                   Yuan Gao, Lili Yao, Ni-Bin Chang and Dingbao Wang\*

3                   Department of Civil, Environmental, and Construction Engineering, University of Central

4                   Florida, Orlando, FL 32816, United States

5                   \*Correspondence to D. Wang, [dingbao.wang@ucf.edu](mailto:dingbao.wang@ucf.edu)

6                   **Abstract**

7                   Prediction of mean annual runoff is of great interest but still poses a challenge in ungauged basins.

8                   The present work diagnoses the prediction in mean annual runoff affected by the uncertainty in

9                   estimated distribution of soil water storage capacity. Based on a distribution function, a water

10                  balance model for estimating mean annual runoff is developed, in which the effects of climate

11                  variability and the distribution of soil water storage capacity are explicitly represented. As such,

12                  the two parameters in the model have explicit physical meanings, and relationships between the

13                  parameters and controlling factors on mean annual runoff are established. The estimated

14                  parameters from the existing data of watershed characteristics are applied to 35 watersheds. The

15                  results showed that the model could capture 88.2% of the actual mean annual runoff on average

16                  across the study watersheds, indicating that the proposed new water balance model is promising

17                  for estimating mean annual runoff in ungauged watersheds. The underestimation of mean annual

18                  runoff is mainly caused by the underestimation of the spatial heterogeneity of soil water storage

19                  capacity due to neglecting the effect of land surface and bedrock topography. ~~A-h~~Higher spatial

20                  variability of soil storage capacity estimated through the Height Above the Nearest Drainage

21                  (HAND) and Topographic Wetness Index (TWI) indicated that topography plays a crucial role in

22                  determining the actual soil water storage capacity. The performance of mean annual runoff

23                  prediction in ungauged basins can be improved by employing better estimation of soil water

24 storage capacity including the effects of soil, topography and bedrock.  
25 It leads to better diagnose of the data requirement for predicting mean annual runoff in ungauged  
26 basins based on a newly developed process-based model finally.

27 **Keywords:** mean annual runoff; ungauged; storage capacity; curve number; soil; topography;  
28 bedrock

29

### 30 1. Introduction

31 Hydrologists have a long-standing interest in mean annual water balance modeling and  
32 prediction. The factors controlling mean annual runoff have been studied in literature. Mean  
33 climate has been identified as the first order control on mean annual runoff and evaporation and it  
34 has been quantified by climate aridity index, which is defined as the ratio between the mean annual  
35 potential evapotranspiration ( $E_p$ ) and precipitation ( $P$ ) (Turc, 1954; Pike, 1964). Other controlling  
36 factors include the temporal variability of climate (Farmer et al., 2003; Troch et al., 2002; Fu and  
37 Wang, 2019), vegetation (Zhang et al., 2001; Donohue et al., 2007; Gentine et al., 2012; Li et al.,  
38 2013), soil (Atkinson et al., 2002; Yokoo et al., 2008; Li et al., 2014), and topography (Woods,  
39 2003; Abatzoglou and Ficklin, 2017). Mean annual runoff or evaporation has been modeled as a  
40 function of climate aridity index and the equation is usually called as Budyko equation (Budyko,  
41 1958). The effects of other factors are represented by including a parameter to Budyko equations  
42 (Fu, 1981; Yang et al., 2008; Wang and Tang, 2014). Among these factors, climate including its  
43 mean and temporal variability, and soil water storage capacity including its mean and spatial  
44 variability are dominant catchment characteristics controlling mean annual runoff, especially for  
45 those catchments dominated by saturation excess  
46 runoff generation (Milly, 1994).

Formatted: Font: Italic

47 Intra- and inter-annual climate variability introduces non-steady state conditions to finer  
48 timescale water balances and the non-steady state effect could propagate to the mean annual runoff.  
49 The effects of seasonal variations of precipitation and potential evaporation on long-term runoff  
50 have been studied in several studies. Milly (1994) showed that seasonality tends to increase mean  
51 annual runoff through a stochastic soil moisture model. The seasonality effects have been  
52 demonstrated through a top-down model by Hickel and Zhang (2006) and a classification study by  
53 Berghuijs et al. (2014). Mean annual water balance also receives impacts from climate variability  
54 at the inter-annual and daily timescales. Li (2014) showed that the inter-annual variability of  
55 precipitation and potential evaporation could increase the mean annual runoff up to 10% based on  
56 a stochastic soil moisture model. Shao et al. (2012) found that daily precipitation with a larger  
57 variation potentially increases mean annual runoff especially in the catchments where infiltration  
58 excess runoff is prevalent. Yao et al. (2020) quantified the relative contribution of daily, monthly  
59 and inter-annual climate variabilities to mean annual runoff and showed that the contribution  
60 decreases, by average, from monthly to inter-annual scale, and then daily scale.

61 Soil water storage capacity is the maximum storage capacity from the land surface to the  
62 bedrock, which exerts a powerful control on mean annual runoff  
63 (Konapala and Mishra, 2016). A smaller soil water storage capacity creates favorable conditions  
64 for runoff generation because the precipitation in excess of the available storage capacity would  
65 be lost as runoff directly, while catchments with a larger soil water storage capacity could hold  
66 more precipitation for evaporation (Sankarasubramanian and Vogel, 2002; Porporato et al., 2004;  
67 Chen et al., 2013). Soil water storage capacity is closely related to vegetation since the root  
68 structure of vegetation could affect soil water storage capacity significantly. Research has  
69 been conducted to reveal the role of soil water storage capacity through the linkage of vegetation

Formatted: Font: Not Italic

70 and model parameter (Yang et al., 2008; Chen and Wang, 2015). Gerrits (2009) developed  
71 equations for transpiration and interception by considering the root zone and interception storage  
72 capacity as two of the most important catchment characteristics affecting evapotranspiration. In  
73 addition to the magnitude of the average soil water storage capacity, the spatial variability of soil  
74 water storage capacity within a catchment also influences precipitation partitioning at the event  
75 scale, and further influences the cumulative runoff at the mean annual scale (Moore, 1985;  
76 Jothityangkoon et al., 2001; Gao et al., 2016). It has also been suggested that the spatial variability  
77 of soil water storage capacity could suppress the actual evaporation because the maximum  
78 evaporation in areas with soil water storage capacity less than  $E_p$  will smaller than  $E_p$ ; therefore,  
79 the average evaporation over the entire catchment is smaller than  $E_p$  even though the average  
80 storage is greater than  $E_p$ , resulting in more runoff generation compared to the situation when the  
81 soil water storage capacity is spatially uniform (Yao et al., 2020)

Formatted: Font: Not Italic

82 .

83 .

84 Therefore, climate variability and soil water storage capacity need to be explicitly  
85 incorporated into the model for predicting mean annual runoff. The effect of climate variability  
86 could be taken into account by driving the model with daily precipitation and potential evaporation  
87 which are usually available. The spatial distribution of soil water storage capacity could be  
88 modelled by a distribution function, and it is usually modelled by the generalized Pareto  
89 distribution (Moore, 1985; Zhao, 1992). The distribution function includes two parameters, i.e.,  
90 the shape parameter and the maximum storage capacity over the watershed. In ungauged basins,  
91 soil water storage capacity and its spatial variability need to be estimated directly from available  
92 data. Gao et al. (2014) adopted the mass curve technique, which has been used for designing the



93 storage capacity of reservoir, to estimate the average water storage capacity of the root zone using  
94 precipitation and potential evaporation data. The shape parameter of the distribution function has  
95 been estimated from soil data (Huang et al., 2003). However, the estimated parameters from these  
96 methods bring much uncertainty in runoff estimation, and the two parameters of the generalized  
97 Pareto distribution are usually estimated by model calibration using observed streamflow data  
98 (Wood et al., 1992; Alipour and Kibler, 2018, 2019).

99 The objective of this paper is to develop a nonparametric mean annual water  
100 balance model for predicting mean annual runoff in ungauged basins, which has not yet been fully  
101 understood (Blöschl et al., 2013). The mean annual water  
102 balance model is forced by daily precipitation and potential evaporation; therefore, the climate  
103 variability at different timescales is represented explicitly in the climate input. The runoff  
104 generation is quantified by a distribution function for describing the spatial distribution of soil  
105 water storage capacity (Wang, 2018). The mean and the shape parameter of the distribution  
106 function need to be estimated from the available data in ungauged basins. Therefore, the model  
107 serves as a diagnosis tool for evaluating the data requirement for estimating soil water storage  
108 capacity. The mean soil water storage capacity is estimated from curve number and climate  
109 because the soil water storage capacity consists of the antecedent soil water storage and the  
110 potential maximum soil moisture retention which can be calculated through SCS curve number  
111 method.

112 The estimation of the shape  
113 parameter is diagnosed in terms of the data requirement including soil, land surface topography,  
114 and bedrock topography. Section 2 introduces the new mean annual water balance model and the

115 study watersheds. Results and discussion are presented in Section 3, followed by Section 4 for  
116 conclusions.

## 117 2. Methodology

### 118 2.1 Mean annual runoff model

119 Climate variability is defined as the temporal variations of the precipitation ( $P$ ) and  
120 potential evapotranspiration ( $E_p$ ), including their intra-monthly, intra-annual, and inter-annual  
121 variations. For example, the deviations of daily  $P$  or  $E_p$  from its monthly mean values are defined  
122 as the intra-monthly variations (Yao et al., 2020). As discussed in the introduction section, the  
123 mean annual runoff model takes daily precipitation and potential evaporation as inputs, therefore,  
124 climate variability is explicitly included in the model.  
125 The developed  
126 model calculates daily soil wetting (infiltration) and evaporation by tracking the soil water  
127 storage. Mean annual runoff is estimated by aggregating the daily values. The daily soil wetting  
128 is calculated using the concept of saturation excess runoff generation by modeling the spatial  
129 variability of soil moisture and soil water storage capacity. To facilitate the parameter estimation  
130 of storage capacity distribution in ungauged basins, the following distribution function is used for  
131 modeling the spatial distribution of storage capacity (Wang, 2018):

$$132 \quad F(C) = 1 - \frac{1}{a} + \frac{C + (1-a)S_b}{a\sqrt{(C+S_b)^2 - 2aS_bC}} \quad (1)$$

133 where  $F(C)$  is the cumulative distribution function (CDF), representing the fraction of the  
134 watershed area for which the soil water storage capacity is equal to or less than  $C$ ;  $a$  is the shape  
135 parameter of the distribution and varies between 0 and 2; and  $S_b$  is the average soil water storage  
136 capacity over the watershed (i.e., the mean of the distribution). As shown in Wang (2018), this

137 distribution function leads to the SCS curve number (SCS-CN) method when the initial storage is  
 138 set to zero. Therefore, there is a linkage between  $S_b$  and the “potential maximum retention after  
 139 runoff begins” in the SCS-CN method, denoted as  $S_{CN}$ .

140 Daily soil wetting and runoff generation is computed as a function of daily precipitation  
 141 ( $P$ ), initial storage ( $S_0$ ),  $a$ , and  $S_b$ . As shown in Wang (2018), the average soil wetting ( $W$ ) is  
 142 computed by:

$$143 \quad W = \frac{P + S_b \sqrt{(m+1)^2 - 2am} - \sqrt{[P + (m+1)S_b]^2 - 2amS_b^2 - 2aS_bP}}{a} \quad (2)$$

144 where  $m = \frac{S_0(2S_b - aS_0)}{2S_b(S_b - S_0)}$ . Setting  $S_0 = 0$  and dividing  $P$  on both sides of Equation (2), a Budyko-  
 145 type equation, representing  $\frac{W}{P}$  as a function of  $\frac{S_b}{P}$ , is obtained (Wang and Tang, 2014), which has  
 146 been used to model long-term soil wetting (Tang and Wang, 2017). Therefore, Equation  
 147 (2) can be interpreted as a non-steady state Budyko equation which accounts for the effect of water  
 148 storage. Daily evaporation ( $E_d$ ) is computed as (Yao et al., 2020):

$$149 \quad E_d = \frac{W + S_0}{S_b} E_p + S_b \frac{\sqrt{(E_p + S_b)^2 - 2aS_bE_p}}{a} \quad (3)$$

150 The first component on the right-hand side of Equation (3),  $\frac{W + S_0}{S_b}$ , is the percentage of  
 151 storage, and the second component is the evaporation for the condition when the entire watershed  
 152 is saturated, i.e., the spatial distribution of soil water storage is same as that of storage capacity  
 153 (Yao et al., 2020). Dividing  $W + S_0$  on both-hand sides, Equation (3) represents  $\frac{E_d}{W + S_0}$  as  
 154 a function of  $\frac{E_p}{S_b}$ , and the function is same as the Budyko-type equation derived by Wang and Tang  
 155 (2014). Mean annual evaporation ( $\bar{E}$ ) is computed by aggregating the daily evaporation, and mean  
 156 annual runoff ( $\bar{Q}$ ) is computed as the difference of mean annual precipitation and evaporation:

157 
$$\bar{E} = \frac{\sum_{y=1}^Y \sum_{d=1}^{D_y} E_d}{Y} \quad (4)$$

158 
$$\bar{Q} = P - \bar{E} \quad (5)$$

159 where,  $Y$  is the number of years, and  $D_y$  is the number of days in  $y^{\text{th}}$  year;  $y$  and  $d$  represent the  
160  $y^{\text{th}}$  year and  $d^{\text{th}}$  day, respectively. Note that the mean annual runoff includes surface runoff and  
161 baseflow, and both are impacted by climate variability (e.g., intra-annual variability) (Berghuijs et  
162 al., 2014; Fan et al., 2007).

Formatted: Font: Times New Roman, 小四, Not Italic

Formatted: Font: Times New Roman, 小四, Check spelling and grammar

163 This mean annual water balance model applies two non-steady Budyko-type equations at the daily

## 164 2.2 Parameter estimation

### 165 2.2.1 Average soil water storage capacity

166 Under a given soil moisture condition, soil water storage capacity is the sum of actual water  
167 storage and the remaining (or effective) storage capacity. The effective storage capacity  
168 corresponding to the normal antecedent moisture condition defined in the SCS-CN method,  $S_{CN}$   
169 (mm), is computed as a function of CN (SCS, 1972; Bartlett et al., 2016):

170 
$$S_{CN} = 25.4(1000/CN - 10) \quad (6)$$

171 where CN is the composite curve number based on land use and land cover (LULC) and  
172 hydrologic soil group (HSG) for each watershed. The LULC data can be obtained from  
173 the National Land Cover Database (Homer et al., 2015), and the HSG data can be extracted from  
174 the Gridded Soil Survey Geographic (gSSURGO) database with a spatial resolution of 10 m  
175 (USDA, 2014). In HSG, soils are assigned to one of the four groups (A, B, C, and D) and three  
176 dual classes (A/D, B/D, and C/D) according to the rate of infiltration when the soils are not  
177 protected by vegetation and receive precipitation from long-duration storms. For the cells  
178 characterized by dual classes, the CN value is calculated as the average of the two CN values  
179 corresponding to the two soil groups.

180 The average soil water storage capacity ( $S_b$ ) is the sum of the actual storage under the  
181 normal condition ( $\bar{S}$ ) and its corresponding effective storage capacity:

$$182 \quad S_b = \bar{S} + S_{CN} \quad (7)$$

183 The physical meaning of  $S_b$  is the mean value of the soil water storage capacity over a watershed  
184 which is defined as the maximum storage from land surface to bedrock in this study rather than  
185 the storage capacity from shallow soils. Since the “normal antecedent moisture” can be interpreted  
186 as the steady-state soil moisture condition,  $\bar{S}$  is the long-term average storage over the watershed.  
187 The values of  $\bar{S}$  for 59 MOPEX (MOdel Parameter Estimation Experiment) watersheds are  
188 estimated based on the long-term water balance model in Yao et al. (2020); and these watersheds  
189 do not include any watersheds studied in this paper. The long-term water balance model used in  
190 their study has a same model structure but the two parameters, i.e., the mean value of the soil water  
191 storage capacity and its shape parameter in the distribution function, were obtained by model  
192 calibration. The ratio between  $\bar{S}$  and  $S_b$  is defined as the long-term storage ratio ( $\frac{\bar{S}}{S_b}$ ). It is found  
193 that the values of  $\frac{\bar{S}}{S_b}$  for all the watersheds were larger than 0.5. As shown in Figure 1,  $\frac{\bar{S}}{S_b}$  has a  
194 linear relationship with the climate aridity index:

$$195 \quad \frac{\bar{S}}{S_b} = -0.46\Phi + 1.2$$

196 (8)

197 where  $\Phi$  is the climate aridity index. Substituting Equations (6) and (7) into  
198 Equation (8), one can estimate the average soil water storage capacity as a function of curve  
199 number and climate aridity index:

$$200 \quad S_b = \frac{S_{CN}}{0.46\Phi - 0.2} \quad (9)$$

### 201 2.2.2 Shape parameter

202 The spatial variability of storage capacity is determined by the spatial distribution of point-  
 203 scale pore space across the watershed. The volume of soil pores at point scale can be determined  
 204 by soil thickness and porosity in different soil layers. The porosity ( $\theta_s$ ) for each layer is calculated  
 205 from the soil bulk density:

$$206 \quad \theta_s(j) = 1 - \frac{\rho_b(j)}{\rho} \quad (10)$$

207 where  $j$  denotes the  $j^{\text{th}}$  soil layer;  $\rho_b(j)$  is the bulk density of the  $j^{\text{th}}$  soil layer;  $\rho$  is the particle  
 208 density (2.65 g/cm<sup>3</sup>). After obtaining the porosity, the point-scale storage capacity can be  
 209 calculated as the following equation (Huang et al., 2003):

$$210 \quad C = \sum_1^n z_j \cdot \theta_s(j) \quad (11)$$

211 where  $C$  is the point-scale soil storage capacity;  $n$  is the number of soil layers;  $z_j$  and  $\theta_s(j)$  are the  
 212 thickness and porosity of the  $j^{\text{th}}$  soil layer, respectively. In the gSSURGO database, the soil  
 213 thickness and bulk density for each layer are available for shallow soil from the land surface to ~  
 214 2 m soil depth.

215 The total soil thickness at each point is the elevation difference from land surface to the  
 216 fresh bedrock. However, the bedrock topography is difficult to obtain especially at the  
 217 watershed scale. Alternatively, it is assumed that the spatial distribution of the actual  
 218 soil water storage capacity is same as the spatial distribution of water storage capacity computed  
 219 from the gSSURGO database. In order to compare the shape parameter evaluated from the soil  
 220 data with its counterparts evaluated from other methods, the point-scale storage capacity is  
 221 normalized with the average storage capacity over the watershed, and Equation (1) is rewritten as:

$$222 \quad F(x) = 1 - \frac{1}{a} + \frac{x+(1-a)}{a\sqrt{(x+1)^2-2ax}} \quad (12)$$

223 where  $x$  is the normalized storage capacity  $\left(\frac{c}{s_b}\right)$  at point scale;  $a$  is the shape parameter describing  
224 the spatial variability of soil water storage capacity. The shape parameter  $a$  is then estimated  
225 by fitting the point-scale storage capacity data obtained from Equation (11).  
226 A nonlinear programming solver using  
227 derivative-free method (i.e., Matlab function “fminsearch”) was used to calculate the optimal  
228 shape parameter by minimizing the root mean square error (RMSE). To demonstrate the  
229 sensitivity of the mean annual runoff to the value of shape parameter, Figure 2 presents mean  
230 annual runoff versus shape parameter based on the mean annual water balance (Yao et al., 2020).  
231 It can be found that mean annual runoff decreases significantly as the shape parameter increases,  
232 especially when shape parameter approaches its upper limit (e.g., 2). The negative relationship  
233 between the mean annual runoff and the shape parameter can be attributed to the fact that the larger  
234 shape parameter indicates that less watershed area has small values of point-scale storage capacity  
235 (Wang, 2018) and more precipitation could be retained underground for evaporation.

### 236 2.3. Study watersheds

237 The estimations of mean annual runoff in 35 watersheds are diagnosed in this paper. The  
238 number of 35 was determined due to the consideration of the data availability including soil  
239 (hydrologic soil group), land cover and land use, DEM as well as the minimum snow effect and  
240 human activities (Wang and Hejazi, 2011), and to keep the efforts of gSSURGO data processing  
241 to a reasonable level while still to have a sufficient number of sample of watersheds. The drainage  
242 area of the watersheds varies from 2044 to 9889 km<sup>2</sup>. Table 1 shows the USGS gauge number and  
243 climate aridity index of these watersheds. The  
244 saturation excess is the dominated runoff generation in these watersheds. Daily  
245 precipitation and streamflow data during 1948 – 2003 are extracted from the MOPEX dataset

246 (Duan et al., 2006), and the daily potential evaporation during this period is calculated based on  
247 the Hargreaves method (Hargreaves and Samani, 1985) by using the daily maximum, minimum,  
248 and mean temperature. The average soil water storage capacity and the shape parameter for these  
249 watersheds are estimated from the available data of climate, LULC, soil, and topography, and the  
250 predictions of mean annual runoff are diagnosed.

### 251 **3. Results and discussion**

#### 252 **3.1. Estimated average soil water storage capacity**

253 The potential maximum retention ( $S_{CN}$ ) is calculated based on the average CN in each  
254 watershed (Table 1). The average CN is computed based on LULC and hydrologic soil group.  
255 For examples, Figure 3a shows the LULC map for the Fox River watershed in Wisconsin and  
256 Figure 3d shows the LULC map for the Spoon River watershed in Illinois. The dominant land  
257 uses are agriculture (49%) and forest (33%) in the Fox River watershed, and agriculture (77%) and  
258 forest (15%) in the Spoon River watershed. The hydrologic soil groups are shown in Figure 3b  
259 (Fox River watershed) and Figure 3e (Spoon River watershed). Given the same LULC, the  
260 hydrologic soil group D is more favorable for runoff generation compared with group A. The  
261 dominant hydrologic soil groups are group A (31%) and group B (19%) in the Fox River watershed,  
262 and group C/D (49%) and group B/D (20%) in the Spoon River watershed. The calculated CN for  
263 each grid cell is shown in Figure 3c (Fox River watershed) and Figure 3f (Spoon River watershed).  
264 The average CN is 61.0 for the Fox River watershed and 78.1 for the Spoon River watershed.  
265 Since the Spoon River watershed has a higher percentage of agricultural land and lower soil  
266 permeability, its average CN is higher than that for the Fox River watershed. Correspondingly,  
267 the calculated  $S_{CN}$  in the Fox River watershed (162 mm) is higher than that in Spoon River



268 watershed (71 mm). The values of  $S_{CN}$  over the study watersheds vary from 56 mm (Auglaize  
269 River watershed) to 182 mm (Chattahoochee River watershed) as shown in Table 1.

270 The average soil water storage capacity is estimated based on the computed  $S_{CN}$  and  
271 climate aridity index shown in Equation (8). For examples, the climate aridity index in the Fox  
272 River watershed is 1.12 which is the same as that in the Spoon River watershed. The estimated  $S_b$   
273 is 721 mm in the Fox River watershed and 314 mm for the Spoon River watershed. As shown in  
274 Table 1, the estimated  $S_b$  varies from 177 mm (Chikaskia River watershed) to 1559 mm  
275 (Chattahoochee River watershed) over the study watersheds. Figure 4a shows the spatial  
276 distribution of the estimated  $S_b$ . Watersheds with higher  $S_b$  are mostly distributed in the eastern  
277 US, where the aridity index is relatively lower than that in the other watersheds.

### 278 3.2. Estimated shape parameter

279 The shape parameter ( $a$ ) for the distribution of soil water storage capacity is estimated  
280 based on the soil data in the gSSURGO database. For examples, the black circles in Figure 5  
281 show the normalized storage capacity for the Fox River watershed (Figure 5a) and the Spoon  
282 River watershed (Figure 5b) based on the soil data in the gSSURGO database. As shown in  
283 Figure 5, the normalize CDF for both watersheds shows an S-shape. The estimated shape  
284 parameter is 1.996 for the Fox River watershed (RMSE = 0.58) and 1.990 for the Spoon River  
285 watershed (RMSE = 1.27) by fitting to the soil data. Higher value of shape parameter indicates  
286 less spatial variability; therefore, the spatial variability in the Spoon River watershed is higher than  
287 that in the Fox River watershed. The mean value of RMSE for the 35 study watersheds is 0.06.  
288 Figure 4b shows the estimated shape parameters for the study watersheds, which vary from  
289 1.830 to 1.998.

### 290 3.3. Diagnosing mean annual runoff prediction

Formatted: Font color: Auto

291 The estimated values of  $S_b$  and  $a$  based on climate, LULC, and soil data are applied to the  
292 mean annual water balance model. The comparison of simulated and observed mean annual runoff  
293 for the study watersheds is shown in Figure 6a. The RMSE for estimated mean annual runoff  
294 is 80 mm/yr. The water balance model captures 88.2% of the mean annual runoff across the 35  
295 study watersheds; therefore, the methods for estimating  $S_b$  and  $a$  based on the available data are  
296 promising for predicting annual runoff in ungauged basins.

297 The water balance model with the estimated values of  $S_b$  and  $a$  underestimates the mean  
298 annual runoff in some watersheds, and the relative underestimation error is 11.8% on average  
299 among all the study watersheds. The underestimation of mean annual runoff could be due to the  
300 biased estimation of the shape parameter. As described in Section 3, the spatial variability of soil  
301 water storage capacity is assumed to be equal with the spatial variability of the pore space in the  
302 shallow soil. The pore space at the point scale is calculated through the porosity and soil thickness.  
303 The thickness of the shallow soil in the gSSURGO database is quite uniformly distributed across  
304 the watershed, i.e., around 2 m; whereas, the actual soil thickness including the weathered bedrock  
305 is the elevation difference between the land surface and fresh bedrock, and can be highly  
306 heterogeneous due to the variable land surface and bedrock topography over the  
307 watershed.

308 To diagnose the effect of land surface and bedrock topography on mean annual water  
309 balance, the shape parameter is calibrated using the observed streamflow. The streamflow data  
310 during 1948-2003 are divided into three periods: 1) the warm-up period (1948-1953); 2) the  
311 calibration period (1954-1973); and 3) the validation period (1974-2003). During the calibration,  
312 the estimated  $S_b$  based on CN is used, and  $a$  is the only free parameter to be calibrated. The  
313 calibration is conducted by minimizing the absolute error of the observed and simulated mean

314 annual runoff through a global optimization method, i.e., Shuffled Complex Evolution Method  
315 (Duan et al., 1992). As shown in Figure 6b, most of the calibrated  $a$  are smaller than the  
316 estimated  $a$  based on soil data only. The performance of predicted mean annual runoff (during the  
317 validation period) is improved with the calibrated shape parameter (Figure 6c). The average of  
318 absolute error for the mean annual runoff is 7.1%.

319 The overestimation of shape parameter based on the soil porosity data underestimates the  
320 area percentage of low soil water storage capacity compared with the  
321 calibrated one as shown in Figure 5a for the Fox River watershed and Figure 5b for the  
322 Spoon River watershed. The slope at the normalized soil water storage capacity around 1 for the  
323 estimated shape parameter is higher than that for the calibrated one. Therefore, the calibrated  
324 shape parameter indicates a larger spatial variability. The underestimation of catchment area with  
325 low soil water storage capacity could be resulted from neglecting the  
326 effect of land surface and bedrock topography which cannot be referred from the soil database  
327 (gSSURGO) where the point-scale soil thickness is around 2 m.

328 To explore the impact of land surface topography on the spatial distribution of soil water  
329 storage capacity, the soil data (i.e., porosity) is combined with the Height Above the Nearest  
330 Drainage (HAND) method proposed by Gao et al. (2019). HAND is the vertical elevation  
331 difference from a point to its nearest drainage point. The distribution of HAND was used for  
332 estimating the shape parameter of the spatial distribution of storage capacity. Therefore, the  
333 HAND method uses land surface topography data only for estimating the shape parameter. In our  
334 analysis, the porosity of the soil beyond the bottom layer in the soil database is assigned with the  
335 same value as the bottom layer. For example, if the HAND for a grid cell is 10.0 m and the porosity  
336 and depth of the bottom soil layer in the gSSURGO database is 0.2 and 2.0 m, respectively, the

337 porosity for the soil from 2.0 m to 10.0 m depth is assigned with 0.2. Finally, the total volume of  
338 pores is calculated for each grid cell based on the soil porosity obtained from the gSSURGO  
339 database and the HAND value based on land surface topography.

340 The control of land surface topography on the hydrologic process has also been widely  
341 quantified through topographic wetness index (TWI) of TOPMODEL (Beven and Kirkby, 1979).  
342 The spatial variability of soil storage capacity based on the TOPMODEL assumption has been  
343 demonstrated as a beneficial representation of the conceptual model (Sivapalan et al., 1997).  
344 Therefore, the heterogeneity of TWI in a catchment was proposed to be a surrogate of the  
345 heterogeneity of the soil storage capacity in this study, and the shape parameter estimated by fitting  
346 TWI against Equation (12) through minimizing the root mean square error (RMSE) for the  
347 Maquoketa River in Iowa was compared with those obtained from other methods.

348 The dashed blue line in Figure 7 shows the porosity-HAND based CDF of normalized  
349 soil water storage capacity for the Maquoketa River in Iowa (gauge #05418500). The stream  
350 initiation threshold used for calculating HAND is 40 km<sup>2</sup> which is 1% of the maximum flow  
351 accumulation (Maidment, 2002). The threshold affects the value of HAND but this is beyond the  
352 scope of this paper. The best fit value of  $a$  for the porosity-HAND based CDF is 1.779, which  
353 overestimates the spatial variability of storage capacity compared with the calibrated shape  
354 parameter ( $a=1.905$ ). This is due to the assumption of the HAND method that the bedrock between  
355 a specific point and its nearest drainage point is horizontal and intercepts with the channel bed.  
356 However, the bedrock topography may have various slopes in a watershed (Troch et al., 2002).  
357 Therefore, the true value of  $a$  (indicated by the calibrated one) potentially falls between the  $a$   
358 obtained from soil data and the  $a$  based on soil and HAND. The bedrock topography from  
359 observation or models is needed to accurately estimate the shape parameter. The dashed dot red

360 line in Figure 7 displays the CDF of the normalized soil storage capacity based on TWI, and the  
361 corresponding value of  $\alpha$  is 1.967. The TWI based  $\alpha$  value also present a larger spatial variability  
362 than that derived from soil data solely, confirming the importance of topography in determining  
363 the heterogeneity of soil water storage capacity. The deviation of the TWI-based  $\alpha$  value from its  
364 calibrated counterpart could be due to the fact that the bedrock topography is not considered in  
365 TWI.

#### 366 **4. Conclusion**

367 A mean annual water balance model based on the concept of saturation excess runoff  
368 generation is used for diagnosing the potential for nonparametric modeling of mean annual runoff  
369 in ungauged basins. The model takes the effect of climate variability into account explicitly since  
370 it is driven by daily precipitation and potential evapotranspiration at the daily time step. The  
371 distribution function, which leads to the SCS curve number method, is used for describing the  
372 spatial distribution of soil water storage capacity. The mean (i.e., average soil water storage  
373 capacity) and the shape parameter (i.e., the spatial variability of soil storage capacity over the  
374 watershed) of the distribution function can be estimated from the available data. Based on the  
375 linkage of the distribution function and the SCS curve number method, a new method based on  
376 the existing observed data of watershed characteristics is proposed for estimating the average soil  
377 water storage capacity. The average soil water storage capacity ( $S_b$ ), as one of the parameters in  
378 the model, was estimated as a function of climate aridity index and curve number which is  
379 calculated based on land cover and soil data.

380 The developed mean annual water balance was applied to diagnose the estimation of shape  
381 parameter ( $\alpha$ ) in this study. The shape parameter, describing the spatial variation of soil water  
382 storage capacity, was first estimated based on the porosity and soil thickness data in the soil

383 database (gSSURGO). The estimated values of  $a$  were tested in 35 watersheds. The results  
384 showed that the model with the estimated values of  $S_b$  and  $a$  underestimated the mean annual  
385 runoff by 11.8% on average over all the study watersheds. The underestimation of runoff is mainly  
386 caused by the underestimation of the spatial heterogeneity of soil thickness over the watershed.  
387 The Height Above the Nearest Drainage (HAND) was then calculated as the total soil thickness  
388 for estimating the total volume of the pore space. The result showed that topography is of great  
389 importance for determining the spatial variability of soil water storage capacity. The estimated  
390 shape parameter from porosity-HAND overestimated the spatial variability of the storage capacity  
391 compared with the calibrated  $a$ , which may result from the assumed bedrock in the HAND method.

392 The Topographic Wetness Index (TWI) based shape parameter further indicated the importance  
393 the topography including the land surface topography and bedrock topography. Future research  
394 will investigate alternative methods for better estimating the spatial variability of soil water storage  
395 capacity over watersheds, and quantify the impacts of vegetation and climate variability (e.g.,  
396 distribution of rainy days, the magnitude and the seasonality of climate variables).

397

398

399

#### 400 **Data availability**

401 The soil and land use and land cover data that support the findings of this study are openly available  
402 at: <https://websoilsurvey.sc.egov.usda.gov/App/WebSoilSurvey.aspx> (Natural Resources  
403 Conservation Services, United States Department of Agriculture), and:  
404 <https://www.mrlc.gov/data?f%5B0%5D=category%3Aland%20cover&f%5B1%5D=region%3A>  
405 conus (National Land Cover Database, United States Geological Survey), respectively.

Field Code Changed

Formatted: Font: (Default) Times New Roman, 小四

406 Daily precipitation, streamflow, and temperature data are available from 1948 to 2003 through the  
407 MOPEX website at [https://hydrology.nws.noaa.gov/pub/gcip/mopex/US\\_Data/](https://hydrology.nws.noaa.gov/pub/gcip/mopex/US_Data/).

Formatted: Hyperlink

Formatted: Font: 小四

#### 409 **Author contributions**

410 Dingbao Wang designed the study, contributed to the methods, results discussion and modified  
411 the text. Yuan Gao quantified the parameters of the model and prepared the manuscript with  
412 contributions from all co-authors. Lili Yao developed the model code, quantified the parameters,  
413 performed the simulations and prepared the manuscript with contributions from all co-authors. Ni-  
414 Bin Chang contributed to the introduction and modified the text.

#### 416 **Competing interests**

417 The authors declare that they have no conflict of interest.

#### 419 **Acknowledgements**

420 This research was funded in part under award CBET-1804770 from National Science Foundation  
421 (NSF) and Florida Department of Transportation (FDOT).

#### 422 **Reference**

423 Abatzoglou, J. T., and Ficklin, D. L.: Climatic and physiographic controls of spatial variability in  
424 surface water balance over the contiguous United States using the Budyko relationship,  
425 Water Resour. Res., 53(9), 7630-7643, <https://doi.org/10.1002/2017WR020843>, 2017.  
426 Alipour, M. H. and Kibler, K. M.: A framework for streamflow prediction in the world's most  
427 severely data-limited regions: test of applicability and performance in a poorly-gauged

428 region of China, *J. Hydrol.*, 557, 41-54, <https://doi.org/10.1016/j.jhydrol.2017.12.019>,  
429 2018.

430 Alipour, M. H. and Kibler, K. M.: Streamflow prediction under extreme data scarcity: a step  
431 toward hydrologic process understanding within severely data-limited regions, *Hydrolog.*  
432 *Sci. J.*, 64(9), 1038-1055, <https://doi.org/10.1080/02626667.2019.1626991>, 2019.

433 Atkinson, S. E., Woods, R. A., and Sivapalan, M.: Climate and landscape controls on water balance  
434 model complexity over changing timescales, *Water Resour. Res.*, 38(12),  
435 1314, <https://doi.org/10.1029/2002WR001487>, 2002.

436 Bartlett, M. S., Parolari, A. J., McDonnell, J. J., and Porporato, A.: Beyond the SCS-CN method:  
437 A theoretical framework for spatially lumped rainfall-runoff response, *Water Resour. Res.*,  
438 52(6), 4608-4627, <https://doi.org/10.1002/2015WR018439>, 2016.

439 Berghuijs, W. R., Sivapalan, M., Woods, R. A., and Savenije, H. H.: Patterns of similarity of  
440 Berghuijs, W. R., Sivapalan, M., Woods, R. A., and Savenije, H. H.: Patterns of similarity  
441 Berghuijs, W. R., Sivapalan, M., Woods, R. A., and Savenije, H. H.: Patterns of similarity  
442 Beven, K. J. and Kirkby, M. J.: A physically-based variable contributing area model of basin  
443 hydrology. *Hydrolog. Sci. J.*, 24(1), 43-69, 1979.

444 Blöschl, P. G., Sivapalan, P. M., Wagener, P. T., Viglione, D. A., and Savenije, H. H.: Runoff  
445 Budyko, M.I.: The Heat Balance of the Earth's Surface, U.S. Dep. of Commer., Washington, D.  
446 C., 1958.

447 Chen, X., Alimohammadi, N., and Wang, D.: Modeling interannual variability of seasonal  
448 evaporation and storage change based on the extended Budyko framework, *Water Resour.*  
449 *Res.*, 49(9), 6067-6078, <https://doi.org/10.1002/wrcr.20493>, 2013.

Formatted: Font: (Default) Times New Roman, 小四,  
Font color: Auto, Pattern: Clear

Formatted: Font: (Default) Times New Roman, 小四,  
Font color: Auto, Pattern: Clear

Formatted: Font: (Default) Times New Roman, 小四,  
Font color: Auto, Pattern: Clear



450 Chen, X. and Wang, D.: Modeling seasonal surface runoff and base flow based on the generalized  
451 proportionality hypothesis, *J. Hydrol.*, 527, 367-379,  
452 <https://doi.org/10.1016/j.jhydrol.2015.04.059>, 2015.

453 Donohue, R. J., Roderick, M. L., and McVicar, T. R.: On the importance of including vegetation  
454 dynamics in Budyko's hydrological model, *Hydrol. Earth Syst. Sci.*, 11, 983-995,  
455 <https://doi.org/10.5194/hess-11-983-2007>, 2007.

456 Duan, Q., Sorooshian, S., and Gupta, V.: Effective and efficient global optimization for conceptual  
457 rainfall-runoff models, *Water Resour. Res.*, 28(4), 1015-1031,  
458 <https://doi.org/10.1029/91WR02985>, 1992.

459 Duan, Q., Schaake, J., Andreassian, V., Franks, S., Goteti, G., Gupta, H. V., Gusev, Y. M., Habets,  
460 F., Hall, A., Hay, L., Hogue, T., Huang, M., Leavesley, G., Liang, X., Nasonova, O. N.,  
461 Noilhan, J., Oudin, L., Sorooshian, S., Wagener, T., and Wood, E. F.: Model parameter  
462 estimation experiment (MOPEX): an overview of science strategy and major results from  
463 the second and third workshops, *J. Hydrol.*, 320, 3-17,  
464 <https://doi.org/10.1016/j.jhydrol.2005.07.031>, 2006.

465 [Fan, Y., Miguez-Macho, G., Weaver, C. P., Walko, R., and Robock, A.: Incorporating water table](#)  
466 [dynamics in climate modeling: 1. Water table observations and equilibrium water table](#)  
467 [simulations, \*J. Geophys. Res.\*, 112, D10125, doi:10.1029/2006JD008111, 2007.](#)

468 Farmer, D., Sivapalan, M., and Jothityangkoon, C.: Climate, soil, and vegetation controls upon the  
469 Fu, B. P.: On the calculation of the evaporation from land surface [in Chinese]. *Sci. Atmos. Sin.*  
470 5, 23-31, 1981.

471 Fu, J. and Wang, W.: On the lower bound of Budyko curve: The influence of precipitation  
472 seasonality, *J. Hydrol.*, 570, 292- 303, <https://doi.org/10.1016/j.jhydrol.2018.12.062>, 2019.

473 Gao, H., Hrachowitz, M., Schymanski, S. J., Fenicia, F., Sriwongsitanon, N., and Savenije, H. H.  
474 G.: Climate controls how ecosystems size the root zone storage capacity at catchment scale,  
475 Geophys. Res. Lett., 41, 7916-7923, <https://doi.org/10.1002/2014GL061668>, 2014.

476 Gao, H., Hrachowitz, M., Sriwongsitanon, N., Fenicia, F., Gharari, S., and Savenije, H. H.:  
477 Accounting for the influence of vegetation and landscape improves model transferability  
478 in a tropical savannah region, Water Resour. Res., 52(10), 7999-8022,  
479 <https://doi.org/10.1002/2016WR019574>, 2016.

480 Gao, H., Birkel, C., Hrachowitz, M., Tetzlaff, D., Soulsby, C., and Savenije, H. H.: A simple  
481 topography-driven and calibration-free runoff generation module, Hydrol. Earth Syst. Sci.,  
482 23, 787-809, <https://doi.org/10.5194/hess-23-787-2019>, 2019.

483 Gentine, P., D'Odorico, P., Lintner, B. R., Sivandran, G., and Salvucci, G.: Interdependence of  
484 climate, soil, and vegetation as constrained by the Budyko curve, Geophys. Res. Lett., 39,  
485 L19404, <https://doi.org/10.1029/2012GL053492>, 2012.

486 Gerrits, A. M. J., Savenije, H. H. G., Veling, E. J. M., and Pfister, L.: Analytical derivation of the  
487 Budyko curve based on rainfall characteristics and a simple evaporation model, Water  
488 Resour. Res., 45, W04403, <https://doi.org/10.1029/2008WR007308>, 2009.

489 Hargreaves, G. H. and Samani, Z. A.: Reference crop evapotranspiration from temperature, Appl.  
490 Eng. Agric., 1(2), 96-99, doi: 10.13031/2013.26773, 1985.

491 Hickel, K. and Zhang, L.: Estimating the impact of rainfall seasonality on mean annual water  
492 balance using a top-down approach, J. Hydrol., 331(3-4), 409-424,  
493 <https://doi.org/10.1016/j.jhydrol.2006.05.028>, 2006.

494 Homer, C. G., Dewitz, J. A., Yang, L., Jin, S., Danielson, P., Xian, G., Coulston, J., Herold, N. D.,  
495 Wickham, J. D., and Megown, K.: Completion of the 2011 National Land Cover Database

496 for the conterminous United States-Representing a decade of land cover change  
497 information, *Photogramm. Eng. Rem. S.*, 81(5), 345-354, 2015.

498 Huang, M., Liang, X., and Liang, Y.: A transferability study of model parameters for the variable  
499 infiltration capacity land surface scheme, *J. Geophys. Res.*, 108(D22), 8864,  
500 <https://doi.org/10.1029/2003JD003676>, 2003.

501 Jothityangkoon, C., Sivapalan, M., and Farmer, D. L.: Process controls of water balance variability  
502 in a large semi-arid catchment: downward approach to hydrological model development,  
503 *J. Hydrol.*, 254(1-4), 174-198, [https://doi.org/10.1016/S0022-1694\(01\)00496-6](https://doi.org/10.1016/S0022-1694(01)00496-6), 2001.

504 [Konapala, G., and Mishra, A. K. : Three-parameter-based streamflow elasticity model: Application](#)  
505 [to MOPEX basins in the USA at annual and seasonal scales., \*Hydrol. Earth Syst. Sci.\*, 20,  
506 \[2545-2556, <https://doi.org/10.5194/hess-20-2545-2016>.\]\(#\)](#)

507 Li, H. Y., Sivapalan, M., Tian, F., and Harman, C.: Functional approach to exploring climatic and  
508 landscape controls of runoff generation: 1. Behavioral constraints on runoff volume, *Water*  
509 *Resour. Res.*, 50, 9300-9322, <https://doi.org/10.1002/2014WR016307>, 2014.

510 Li, D., Pan, M., Cong, Z., Zhang, L., and Wood, E. Vegetation control on water and energy balance  
511 within the Budyko framework, *Water Resour. Res.*, 49, 969-976,  
512 <https://doi.org/10.1002/wrcr.20107>, 2013.

513 Li, D.: Assessing the impact of interannual variability of precipitation and potential evaporation  
514 on evapotranspiration, *Adv. Water Resour.*, 70, 1-11,  
515 <https://doi.org/10.1016/j.advwatres.2014.04.012>, 2014.

516 Maidment, D. R. (Ed.): *ArcHydro: GIS for Water Resources*, ESRI Press, Redlands, Calif., 2002.

517 Milly, P. C. D.: Climate, soil water storage, and the average annual water balance, *Water Resour.*  
518 *Res.*, 30(7), 2143-2156, <https://doi.org/10.1029/94WR00586>, 1994.

519 Moore, R. J.: The probability-distributed principle and runoff production at point and basin scales,  
520 Hydrolog. Sci. J., 30(2), 273-297, <https://doi.org/10.1080/02626668509490989>, 1985.

521 Pike, J. G.: The estimation of annual runoff from meteorological data in a tropical climate, J.  
522 Hydrol., 12, 2116–2123, [https://doi.org/10.1016/0022-1694\(64\)90022-8](https://doi.org/10.1016/0022-1694(64)90022-8), 1964.

523 Porporato, A., Daly, E., and Rodriguez-Iturbe, I.: Soil water balance and ecosystem response to  
524 climate change, Am. Nat., 164(5), 625–632, <https://doi.org/10.1086/424970>, 2004.

525 Sankarasubramanian, A., and Vogel, R. M.: Annual hydroclimatology of the United States, Water  
526 Resour. Res., 38(6), 1083, <https://doi.org/10.1029/2001WR000619>, 2002.

527 SCS.: Hydrology, National Engineering Handbook, Supplement A, Section 4, Chapter 10. Soil  
528 Conservation Service, US Department of Agriculture, Washington, DC., 1972.

529 Shao, Q., Traylen, A., and Zhang, L.: Nonparametric method for estimating the effects of climatic  
530 and catchment characteristics on mean annual evapotranspiration, Water Resour. Res., 48,  
531 W03517, <https://doi.org/10.1029/2010WR009610>, 2012.

532 Tang, Y. and Wang, D.: Evaluating the role of watershed properties in long-term water balance  
533 through a Budyko equation based on two-stage partitioning of precipitation, Water Resour.  
534 Res., 53, 4142–4157, <https://doi.org/10.1002/2016WR019920>, 2017.

535 Troch, P., Loon, E. V., and Hilberts, A.: Analytical solutions to a hillslope-storage kinematic wave  
536 equation for subsurface flow, Adv. Water Resour., 25(6), 637-649,  
537 [https://doi.org/10.1016/S0309-1708\(02\)00017-9](https://doi.org/10.1016/S0309-1708(02)00017-9), 2002.

538 Troch, P. A., Carrillo, G., Sivapalan, M., Wagner, T., and Sawicz, K.: Climate-vegetation-soil  
539 interactions and long-term hydrologic partitioning: Signatures of catchment co-evolution,  
540 Hydrol. Earth Syst. Sci., 17, 2209-2217, <https://doi.org/10.5194/hess-17-2209-2013>, 2013.

541 Turc, L.: Le bilan d'eau des sols: Relation entre les precipitations, l'évaporation et l'écoulement,  
542 Ann. Agron., Serie A 5, 491–595, 1954.

543 USDA: Gridded Soil Survey Geographic (gSSURGO) Database User Guide, U. S. Dep. of Agric.,  
544 Nat. Resour. Conserv. Serv., Washington, D. C., 2014.

545 Wang, D. and Hejazi, M.: Quantifying the relative contribution of the climate and direct human  
546 impacts on mean annual streamflow in the contiguous United States, Water Resour. Res.,  
547 47, W00J12, <https://doi.org/10.1029/2010WR010283>, 2011.

548 Wang, D. and Tang, Y.: A one-parameter Budyko model for water balance captures emergent  
549 behavior in Darwinian hydrologic models, Geophys. Res. Lett., 41, 4569–4577,  
550 <https://doi.org/10.1002/2014GL060509>, 2014.

551 Wang, D.: A new probability density function for spatial distribution of soil water storage capacity  
552 leads to SCS curve number method, Hydrol. Earth Syst. Sci., 22, 6567–6578,  
553 <https://doi.org/10.5194/hess-22-6567-2018>, 2018.

554 Wood, E. F., Lettenmaier, D. P., and Zartarian, V. G.: A land-surface hydrology parameterization  
555 with subgrid variability for general circulation models, J. Geophys. Res., 97(D3), 2717-  
556 2728, <https://doi.org/10.1029/91JD01786>, 1992.

557 Woods, R.: The relative roles of climate, soil, vegetation and topography in determining seasonal  
558 and long-term catchment dynamics, Adv. Water Resour. Res., 37, 701-708,  
559 [https://doi.org/10.1016/S0309-1708\(02\)00164-1](https://doi.org/10.1016/S0309-1708(02)00164-1), 2003.

560 Xing, W., Wang, W., Shao, Q., and Yong, B.: Identification of dominant interactions between  
561 climatic seasonality, catchment characteristics and agricultural activities on Budyko-type  
562 equation parameter estimation, J. Hydrol., 556, 585-599,  
563 <https://doi.org/10.1016/j.jhydrol.2017.11.048>, 2018.

564 Yang, H., Yang, D., Lei, Z., and Sun, F.: New analytical derivation of the mean annual water-  
565 energy balance equation, *Water Resour. Res.*, 44, W03410,  
566 <https://doi.org/10.1029/2007WR006135>, 2008.

567 Yao, L., Libera, D., Kheimi, M., Sankarasubramanian, A., and Wang, D.: The roles of climate  
568 forcing and its variability on streamflow at daily, monthly, annual, and long-term scales,  
569 *Water Resour. Res.*, <https://doi.org/10.1029/2020WR027111>, 2020.

570 Yokoo, Y., Sivapalan, M., and Oki, T.: Investigating the roles of climate seasonality and landscape  
571 characteristics on mean annual and monthly water balances, *J. Hydrol.*, 357(3-4), 255-269,  
572 <https://doi.org/10.1016/j.jhydrol.2008.05.010>, 2008.

573 Zhang, L., Dawes, W. R., and Walker, G. R.: Response of mean annual evapotranspiration to  
574 vegetation changes at catchment scale, *Water Resour. Res.*, 37, 701–708,  
575 <https://doi.org/10.1029/2000WR900325>, 2001.

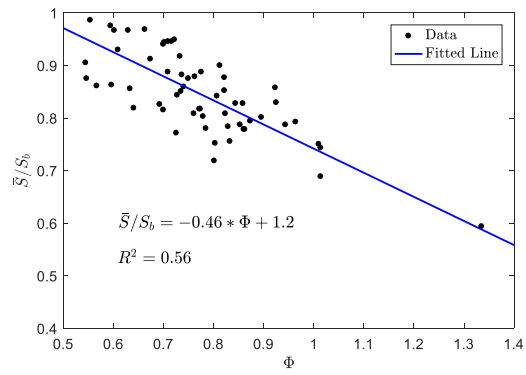
576 Zhao, R. J.: The Xinanjiang model applied in China, *J. Hydrol.*, 135(1–4), 371–381,  
577 [https://doi.org/10.1016/0022-1694\(92\)90096-E](https://doi.org/10.1016/0022-1694(92)90096-E), 1992.

578

579 Table 1: The USGS gage stations, climate aridity index, the estimated potential maximum  
580 retention of curve number method ( $S_{CN}$ ), and the average soil water storage capacity ( $S_b$ ) for the  
581 study watersheds.

Index	Station Name	State	USGS Gauge Number	Climate Aridity Index	$S_{CN}$ (mm)	$S_b$ (mm)
1	Susquehanna River	NY	01503000	0.69	100	862
2	Chemung River	NY	01531000	0.84	95	518
3	Juniata River	PA	01567000	0.85	134	714
4	Rappahannock River	VA	01668000	0.85	152	792
5	Yadkin River	NC	02116500	0.71	153	1221
6	Chattahoochee River	GA	02339500	0.69	182	1559
7	Escambia River	FL	02375500	0.73	143	1075
8	Allegheny River	NY	03011020	0.68	153	1369
9	New River	VA	03168000	0.69	177	1494
10	Great Miami River	OH	03274000	0.89	63	301
11	Eel River	IN	03328500	0.92	68	304
12	East Fork White River	IN	03364000	0.83	68	378
13	Little Wabash River	IL	03381500	0.96	68	279
14	Fox River	WI	04073500	1.12	162	520
15	Auglaize River	OH	04191500	0.98	56	225
16	Maquoketa River	IA	05418500	1.19	72	209
17	Wapsipinicon River	IA	05422000	1.16	69	210
18	Rock River	WI	05430500	1.11	98	316
19	Pecatonica River	IL	05435500	1.11	66	214
20	Kishwaukee River	IL	05440000	1.03	70	255
21	Green River	IL	05447500	1.10	75	247
22	Iowa River	IA	05454500	1.18	65	191
23	Cedar River	IA	05458500	1.17	65	193
24	Kankakee River	IL	05520500	0.93	101	448
25	Fox River	IL	05552500	1.04	88	321
26	Spoon River	IL	05570000	1.12	71	227
27	Kaskaskia River	IL	05592500	0.99	67	263
28	Blue River	KS	06884400	1.70	74	127
29	Thompson River	MO	06899500	1.16	65	195
30	Meramec River	MO	07019000	0.95	109	460
31	Chikaskia River	OK	07152000	1.82	77	121
32	Neosho River	KS	07183000	1.42	63	140
33	Deep Fork River	OK	07243500	1.40	87	197
34	Neches River	TX	08033500	1.14	174	540
35	Elm Fork Trinity River	TX	08055500	1.63	87	159

582  
583



584

585 Figure 1: The degree of saturation ( $\frac{\bar{S}}{S_b}$ ) under long-term average climate versus climate aridity  
 586 index ( $\Phi$ ).

587 Figure 2: The sensitivity of the mean annual runoff ( $Q$ ) to the value of the shape parameter ( $a$ ).

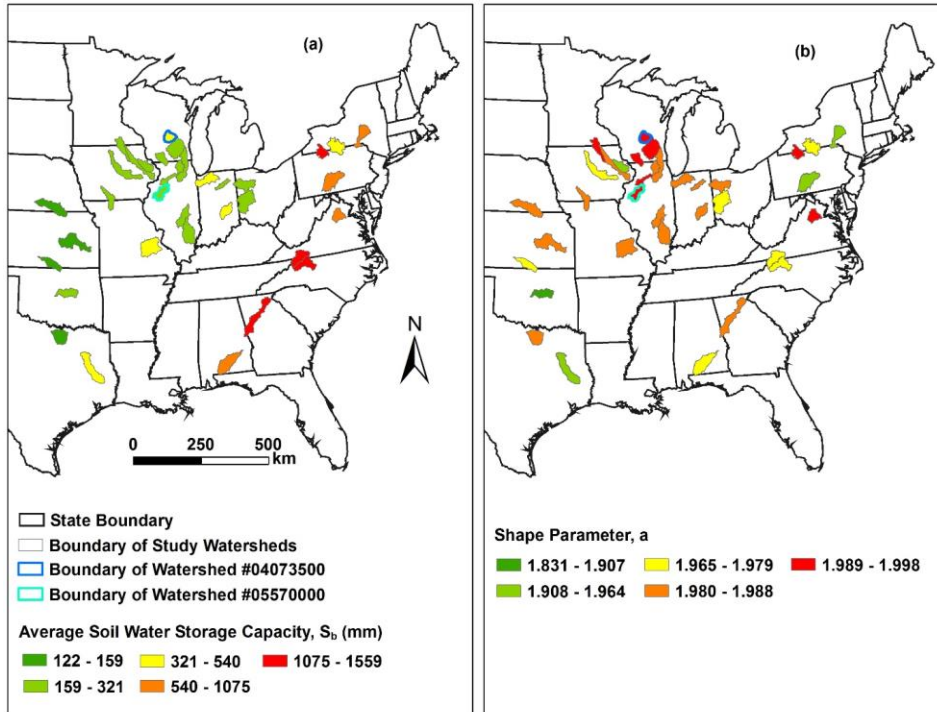
588



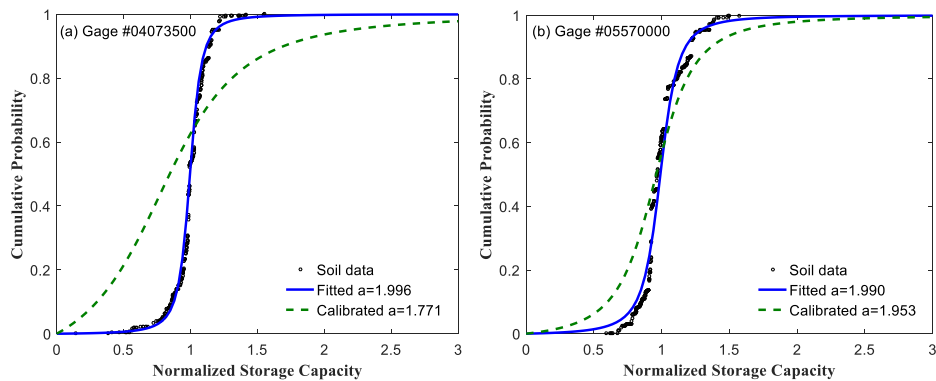
590 Figure 3: The spatial distribution of land use and land cover for Fox River watershed in  
591 Wisconsin (a) and Spoon River watershed in Illinois (d), the hydrologic soil groups for Fox  
592 River watershed (b) and Spoon River watershed (e), and the curve numbers for Fox River  
593 watershed (c) and Spoon River watershed (f).

594

589



595  
 596 Figure 4: The estimated average soil water storage capacity ( $S_b$ ) as a function of  $S_{CN}$  and climate  
 597 aridity index (a) and shape parameter from soil data (b).  
 598



599  
 600 Figure 5: The estimated shape parameter for the spatial distribution of soil water storage capacity  
 601 based on soil data and the calibrated shape parameter based on mean annual water balance in the  
 602 Fox River watershed (a) and the Spoon River watershed (b).

603

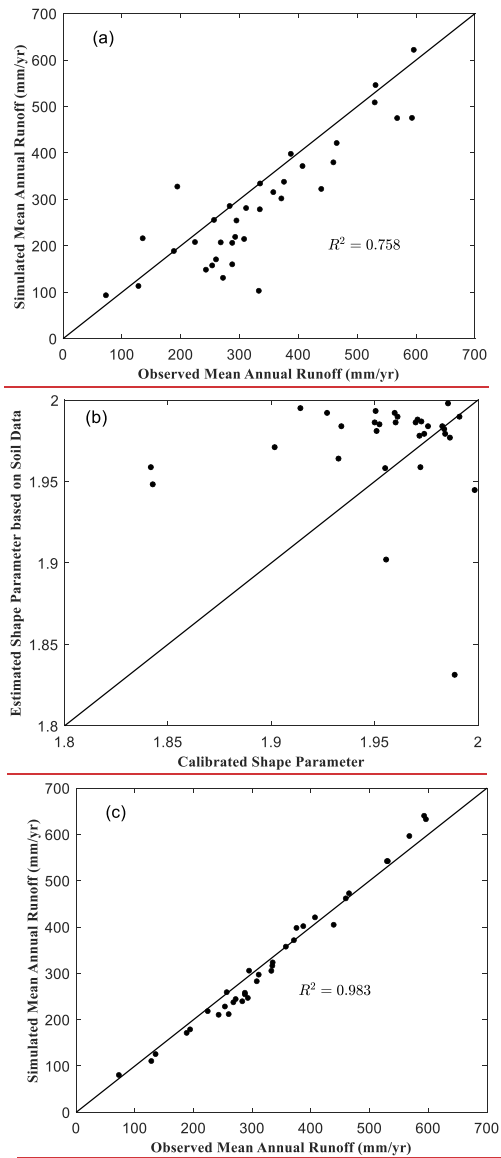
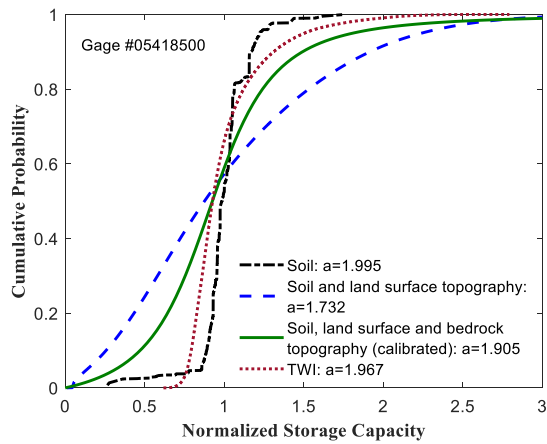


Figure 6: (a) Observed versus simulated mean annual runoff using shape parameter based on soil data; (b) Soil data-based versus calibrated shape parameter; and (c) Observed versus simulated mean annual runoff using shape parameter based on calibration.



611

612 Figure 7: The effects of soil, land surface topography, bedrock topography, and topographic  
 613 wetness index (TWI) on the shape parameter of the spatial distribution of soil water storage  
 614 capacity.

615